View metadata, citation and similar papers at core.ac.uk
brought to you by CORE
provided by IntechOpen

We are IntechOpen, the world's leading publisher of Open Access books Built by scientists, for scientists

4,800
Open access books available

122,000
International authors and editors

135M
Downloads

154
Countries delivered to

Our authors are among the

TOP 1%
most cited scientists

12.2%
Contributors from top 500 universities

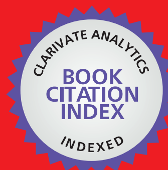

WEB OF SCIENCE™

Selection of our books indexed in the Book Citation Index in Web of Science™ Core Collection (BKCI)

Interested in publishing with us?
Contact book.department@intechopen.com

Numbers displayed above are based on latest data collected.
For more information visit www.intechopen.com

6

The Use of Electron Probe MicroAnalysis to Determine the Thickness of Thin Films in Materials Science

Frédéric Christien, Edouard Ferchaud,
Pawel Nowakowski and Marion Allart
Polytech'Nantes, University of Nantes
France

1. Introduction

Electron Probe MicroAnalysis (EPMA) was born around 1950 when Raymond Castaing, a French graduate student working under the supervision of André Guinier, built his first microanalyser (Castaing & Guinier, 1950; Castaing, 1951; Grillon & Philibert, 2002). The principle of EPMA is to bombard the sample surface with a focused electron beam and to collect the X-rays emitted from the sample. The X-rays are dispersed using Bragg diffraction on a mobile monochromator, which enables to get the whole X-ray spectrum from zero to more than 10 keV. The technique of dispersion is called WDS (Wavelength Dispersive X-ray Spectroscopy). The spectrum is made of continuous background (Bremstrahlung emission) and characteristic peaks, which allow elemental qualitative and quantitative analysis of the material. EPMA-WDS can be carried out in dedicated instruments called "microprobes" (usually fitted with 4 WDS spectometers) or in high current Scanning Electron Microscopes (SEM) equipped with one single WDS spectrometer.
More recently, Energy Dispersive X-ray Spectroscopy has been developed and has nowadays become a cheap and widespread technique. Most SEM in materials science laboratories are equipped with an EDS spectrometer. EPMA-EDS performances are far below those of EPMA-WDS with regards to sensitivity and spectral resolution, although it can achieve very good qualitative and quantitative results in many cases.
EPMA quantification of the sample composition is usually possible by using a standard material of known composition. Unfortunately there is in general no direct proportionality between the concentration of an element and the X-ray emission intensity (peak height) coming from this element. Since the early years of EPMA, many models have been proposed in the literature to correlate the concentration of an element and the associated X-ray emission intensity: ZAF (Philibert & Tixier, 1968), MSG (Packwood & Brown, 1981), PAP and XPP (Pouchou & Pichoir, 1987; Pouchou et al., 1990)… The XPP model (implemented in several microanalysis software packages) has now reached a good level of maturity and reliability, even in difficult situations involving light elements and strong bulk absorption. It is based on an accurate calculation of the $\xi(\rho z)$ curve, which describes the depth-dependence of the X-ray emission intensity of a particular line in the sample. In EPMA analysis of

homogeneous bulk samples, the correlation between X-ray emission intensity and the concentration of an element A in the sample is given by:

$$\frac{I}{I_{Std}} = \frac{X}{X_{Std}} \frac{\int_{\rho z=0}^{\infty} \xi(\rho z)\, d\rho z}{\int_{\rho z=0}^{\infty} \xi_{Std}(\rho z)\, d\rho z} \tag{1}$$

where I is the X-ray intensity of a particular line of element A (for example Kα), I_{Std} is the intensity of the same line measured on a standard material containing a known and homogeneous concentration of element A, z is the depth (cm), ρ is the material density (g cm^{-3}), ρz is the mass thickness (g cm^{-2}), i.e. the mass per unit area of a layer of thickness z, X is the weight fraction of element A in the sample, X_{Std} is the weight fraction of element A in the standard material, and $\xi(\rho z)$ and $\xi_{Std}(\rho z)$ are dimensionless functions that describe the depth distribution of the chosen X-ray line emerging intensity respectively for the sample and for the standard material. The ξ functions depends on the X-ray line chosen for analysis, the matrix composition, the beam voltage and the orientation of the sample surface with respect to the primary beam and the spectrometer. For example, Fig. 1 shows the ξ functions for the palladium Lα line calculated using the XPP model for different matrix compositions (pure palladium and pure nickel) and different accelerating voltages (5, 10 and 20 kV). The calculation was made using the Stratagem™ software (http://www.samx.com) in which the XPP model is implemented (Pouchou, 1993). The influence of matrix composition and beam voltage on the ξ function is demonstrated.

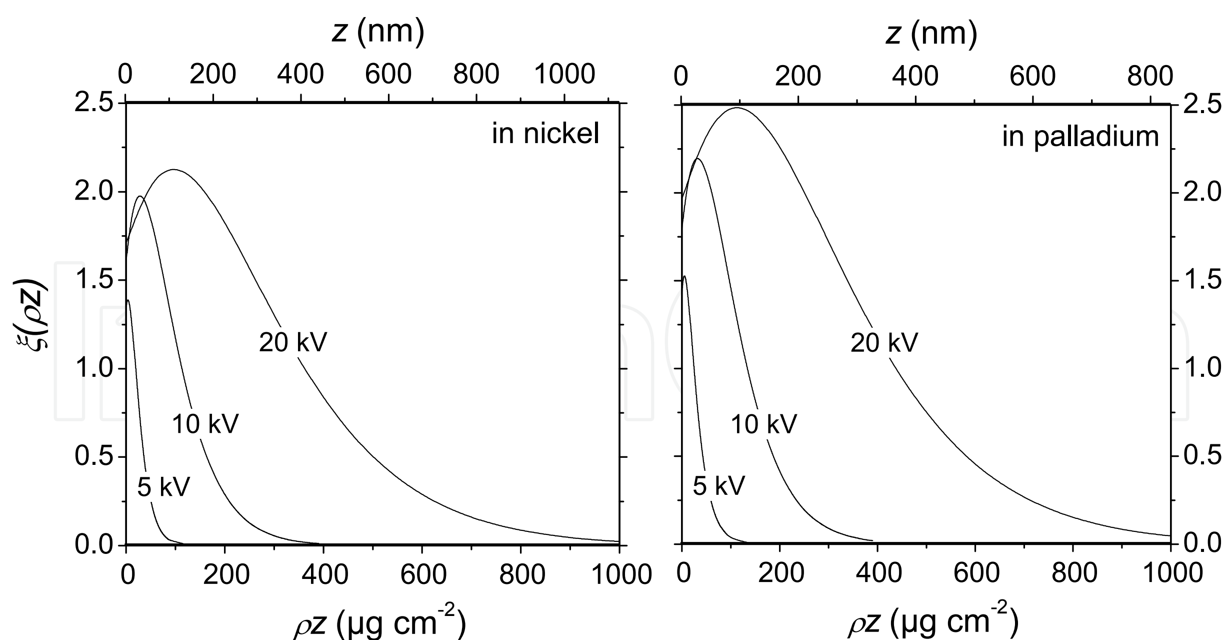

Fig. 1. ξ functions calculated using the XPP model for the palladium Lα line in pure palladium and in pure nickel (containing traces of palladium) at 5, 10 and 20 kV.

From Eq. (1), the correlation between elemental weight fraction and X-ray emission intensity can be determined. Let us consider for example the simple case of a nickel-palladium binary

alloy (this system was considered here because nickel and palladium are totally miscible in the solid state and it is possible to get homogenous Ni-Pd alloys of any composition from pure nickel to pure palladium). Fig. 2 shows the composition dependence of the Pd Lα k-ratio (I / I_{Std}) at 20 kV. The standard material was assumed to be pure palladium here. It can be observed from Fig. 2 that there is no simple proportionality between the Pd Lα k-ratio and the Pd weight fraction. The reason for this is that the ξ function in Eq. (1) depends on the composition.

In general, the composition of a sample analysed by EPMA is not known a priori. It is then not possible to accurately calculate the ξ function, which is needed to correlate the elemental weight fraction and the k-ratio using Eq. (1). An iterative calculation is then needed: in a first step, the elemental weight fraction is assumed equal to the measured k-ratio (1st iteration), which enables to do a first estimation of the ξ function. Then, the elemental weight fraction can be re-estimated using Eq. (1) (2nd iteration). This iterative process is carried out again until it converges to the correct value of the weight fraction (in most cases, a few iterations are sufficient).

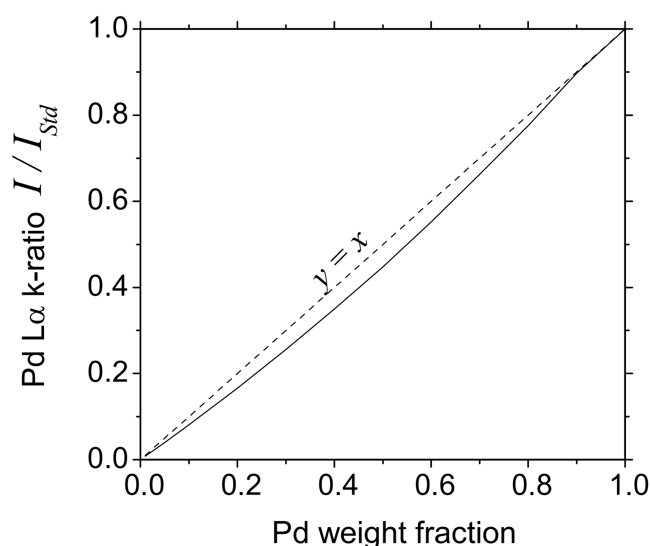

Fig. 2. Composition dependence of the Pd Lα k-ratio (I / I_{Std}) in the Ni-Pd system at 20 kV calculated from Eq. (1).

EPMA is usually presented as a "bulk" analysis technique, as the typical depth of analysis is about 1 μm. It should be mentioned that this 1 μm depth of analysis is only "typical" as it actually strongly depends on both the beam voltage and on the material density (see Fig. 1). Furthermore, EPMA is also very sensitive to "surface" composition and can be used to derive quantitative data such as the thickness and composition of very thin films, down to the monolayer range. The "difficulty" of EPMA applied to thin films is that the probed volume is larger than the film thickness. Since the late eighties, dedicated models have been proposed to overcome that difficulty and to derive thin film thicknesses and compositions from simple and non destructive EPMA measurements (Bastin et al., 1990; Pouchou & Pichoir, 1991; Pouchou, 1993; Pouchou & Pichoir, 1993; Staub et al., 1998; Llovet & Merlet, 2010).

It can be observed nevertheless that EPMA has remained rather underused for the study of thin films with regards to its good sensitivity and quantitative capabilities, real "surface" techniques such as Auger spectroscopy or XPS being often preferred to EPMA. The aim of this paper is to demonstrate the quantitative capabilities of EPMA (associated with either EDS or WDS) for the thickness determination of thin films in materials science.

2. EPMA-EDS: A fast, cheap and simple tool for the characterization of surface thin films from 10 to 1000 nm

2.1 Principle

Let us consider a simple example: a substrate of pure nickel coated with a pure copper layer whose thickness is smaller than the depth of analysis (Fig. 3). In that situation, both nickel and copper X-rays are detected on the EDS spectrum. Assuming that the standard material is pure copper, the Cu k-ratio is given by:

$$\frac{I}{I_{Std}} = \frac{\int_{\rho z=0}^{\mu} \xi(\rho z)\, d\rho z}{\int_{\rho z=0}^{\infty} \xi_{Std}(\rho z)\, d\rho z} \tag{2}$$

where μ is the copper film mass thickness (g cm^{-2}). $\xi(\rho z)$ and $\xi_{Std}(\rho z)$ describe the Cu Kα emission respectively in the Cu/Ni stratified sample and in the standard material (pure copper). Fig. 4 shows the beam voltage dependence of the Cu Kα line k-ratio for several copper mass thicknesses μ. The calculation was carried out using the Stratagem™ software (http://www.samx.com) based on the XPP model (Pouchou, 1993). In such a simple situation (film of known composition on a substrate of known composition), a single voltage approach is sufficient, i.e. μ can be determined from the k-ratio measured at one voltage only. The voltage must be high enough so that the depth of analysis should be higher than the film thickness, otherwise the k-ratio is always equal (or close) to 1 no matter how thick the film is, and the determination of μ is not possible.

Once μ is determined, the copper thickness can be worked out from Eq. (3), assuming that the density ρ (g cm^{-3}) of the film is known:

$$e = \frac{\mu}{\rho} \tag{3}$$

Examples of thin film thickness determination by EPMA-EDS are given in the following sections. Unless otherwise stated, the experimental data were acquired on a Leo S440 SEM equipped with an INCA EDS system from Oxford Instruments.

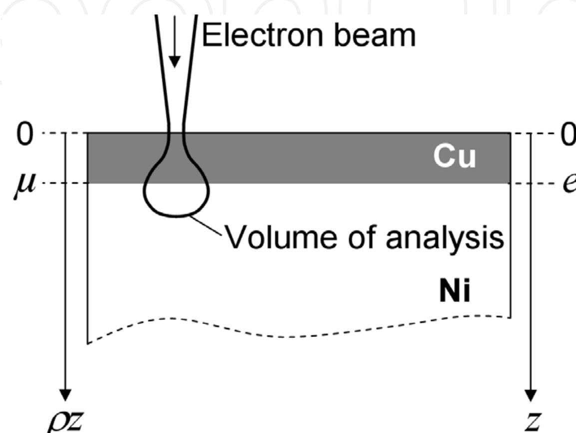

Fig. 3. Principle of surface thin film analysis by EPMA-EDS or EPMA-WDS.

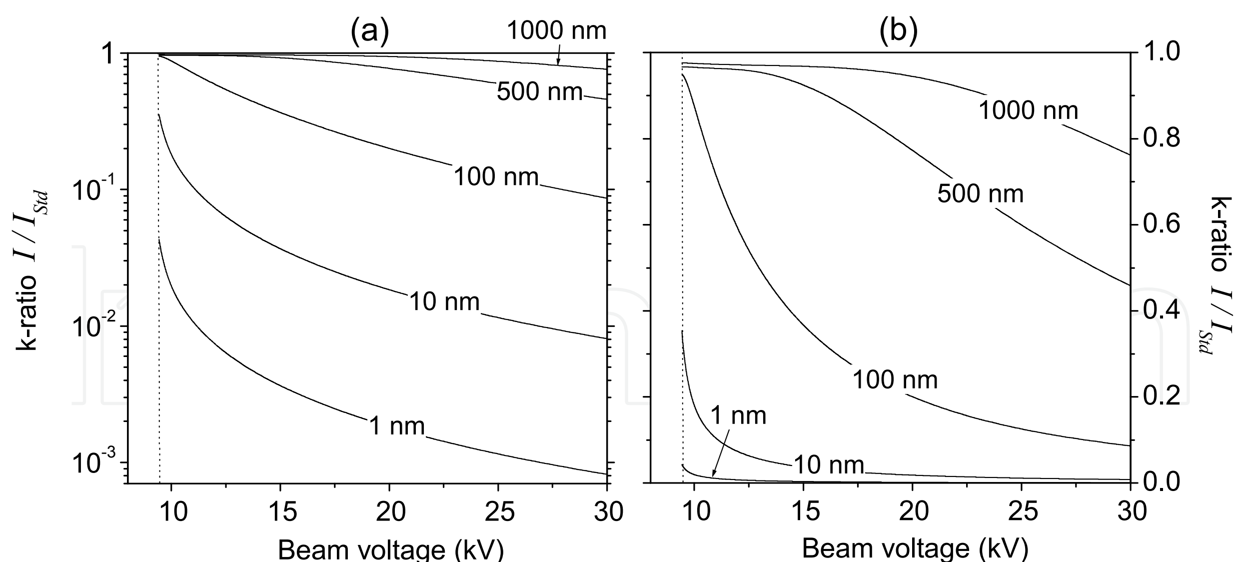

Fig. 4. Beam voltage dependence of Cu Kα k-ratio for various thicknesses of copper deposited on a nickel substrate. (a) logarithmic k-ratio scale. (b) linear k-ratio scale. The dotted vertical line is the copper K level energy below which no Kα emission is observed.

2.2 EPMA-EDS determination of alumina thickness on aluminium samples

Aluminium is a highly oxidizable metal: any aluminium sample is always covered by an alumina (Al_2O_3) layer. EPMA-EDS was used here to determine the alumina thickness on two aluminium samples. The first one was annealed at 500°C under air and a quite thick oxide layer is expected. The second one was stripped using nitric acid. EPMA-EDS analyses were carried out at 20 kV on 20×20 µm areas (rastering beam) throughout the aluminium sample.

Fig. 5a shows the typical EDS spectra measured on both samples. The effect of stripping on the oxide layer and hence the oxygen Kα intensity is clearly demonstrated. The case depicted here is simple (film of known composition on a substrate of known composition) and a single voltage approach was used to determine the oxide layer. The quantification equation is the same as Eq. (2). Ten EDS spectra were acquired on each sample and an average oxygen k-ratio was determined using an Al_2O_3 standard material. Fig. 5b shows the oxygen Kα k-ratio measured at 20 kV for the two samples, as well as the corresponding oxide mass thickness μ determined from Eq. (2) using the Stratagem™ software, and the oxide thickness e calculated from Eq. (3) assuming an alumina density $\rho = 3.96$ g cm^{-3} (Bauccio, 1994). The oxide mass thicknesses found on the annealed sample and on the stripped one are 18.2 µg cm^{-2} and 4.0 µg cm^{-2} respectively, which corresponds to thicknesses of 46 nm and 10 nm.

It is clear from the spectra shown in Fig. 5a that even for an oxide layer as thin as 10 nm, the peak-to-background ratio of oxygen Kα line is still about one, which is undoubtedly above the limit of detection of EDS.

To ensure the reliability of the EPMA-EDS thickness measurements, XPS depth profiling was undertaken on the annealed aluminium using a ThermoVG Thetaprobe spectrometer equipped with a hemispherical analyser and a monochromatic AlKα primary beam (spot diameter of 400 µm). The sputtering sequences were carried out using 3 keV argon ions with an incidence angle of 45° onto a 4 mm^2 rastered area with a 9 A cm^{-2} current density. Both oxide and metal components of the Al2p peak were acquired over sputtering time. Sputtering time was converted to depth using a sputtering rate previously measured on

another aluminium sample. The depth profiles are shown in Fig. 6. No metal aluminium peak is detected within the first ~40 nm, which corresponds to the oxide thickness (the very smooth transition from pure oxide to pure metal, i.e. from ~40 to >~500 nm depth, observed in Fig. 6 is due to the sample roughness). It can be concluded that the oxide layer thickness determined on the annealed aluminium by the two techniques are in very good agreement: ~40 nm and 46 nm by XPS and EPMA-EDS respectively.

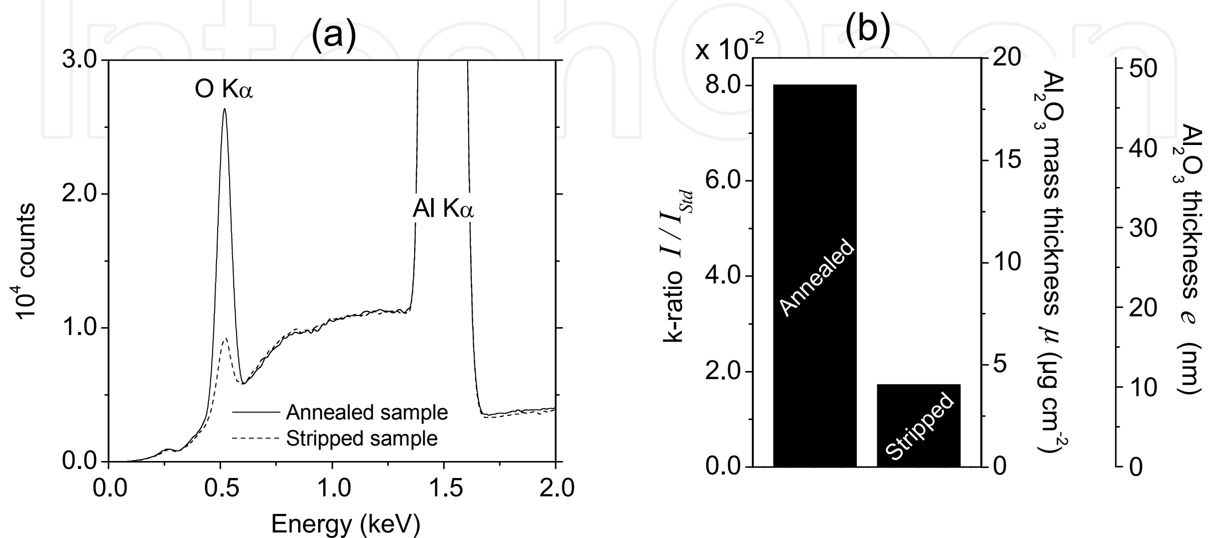

Fig. 5. (a) EDS spectra acquired on aluminium samples at 20 kV. The first sample was annealed at 500°C in air. The second one was stripped in nitric acid. (b): O Kα k-ratio (I / I_{Std}), oxide mass thickness (μ) and oxide thickness (e) measured on the same two aluminium samples by EDS.

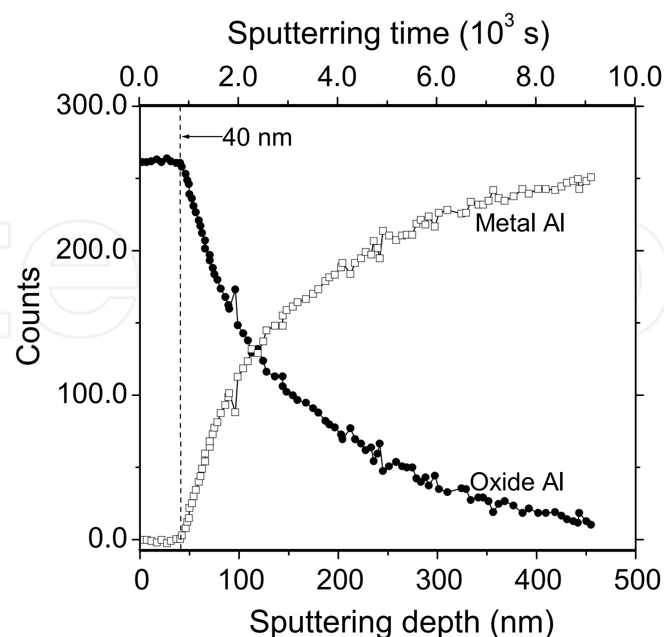

Fig. 6. Confirmation of the alumina thickness on the annealed aluminium by XPS depth profiling. A thickness of ~40 nm is found.

2.3 EPMA determination of gallium thickness on rough gallium-coated aluminium samples

The second example deals with gallium "thick" films deposited on aluminium substrates for brazing applications (Ferchaud, 2010). Solid gallium films were obtained by vapour deposition under vacuum. The typical film surface morphology is shown in Fig. 7a. It can be observed that the film thickness is not homogeneous at the micrometer scale. Thirteen aluminium samples (4x10x40 mm^3) were coated with gallium using different deposition times. For each sample, the Ga film thickness was determined from the film mass measured using a high precision balance (0.01 mg) and from EPMA-EDS analysis. The EPMA-EDS analysis conditions were the same as those depicted in the previous section. Fig. 7b is a comparison of the gallium thicknesses determined by the two techniques. It can be observed that the EPMA-EDS measurements are slightly underestimated (within ~20%) with respect to the thicknesses determined from the film mass. That discrepancy could be due to the gallium film being partly oxidized, in which case the difference between the two techniques would correspond to the oxygen mass in the film. Anyway, it can be observed that the agreement between the two techniques is good although the conditions of EPMA-EDS analyses are far from ideal because of the high surface roughness.

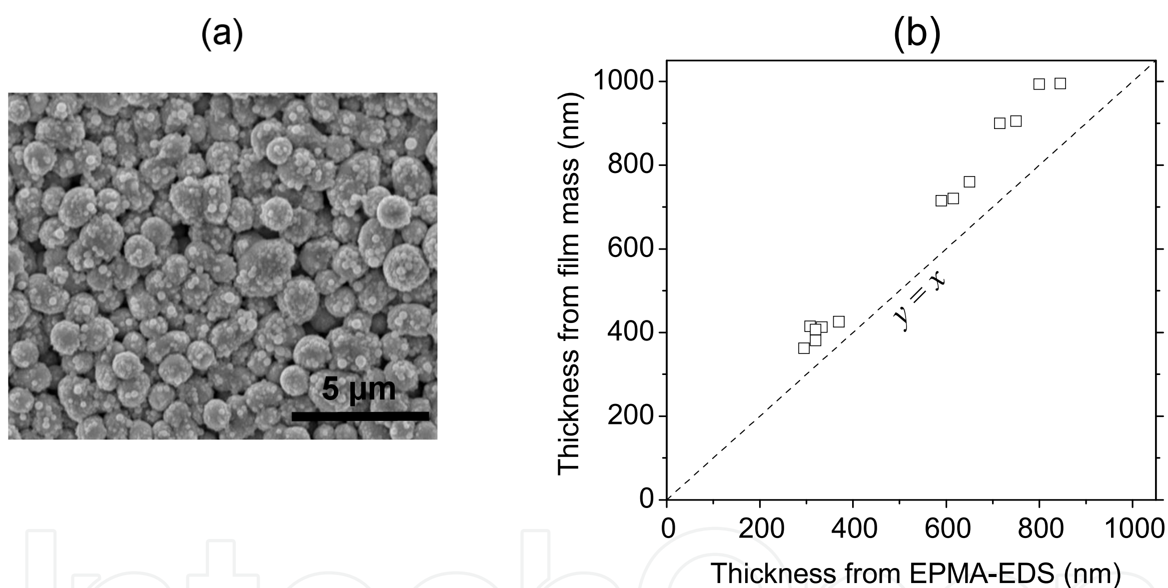

Fig. 7. (a) Typical SEM morphology of the gallium film vapour deposited on aluminium substrates. (b) Comparison of the gallium thickness determined for thirteen aluminium samples from film mass and from EPMA-EDS analysis.

2.4 EDS versus WDS

EPMA-WDS is known to achieve better quantitative results than EPMA-EDS. It is interesting to compare the two techniques with regards to the analysis of thin films. Four copper layers of various thicknesses were electro-deposited on nickel substrates. The copper thickness was determined using both EPMA-EDS and EPMA-WDS at 20 kV. The WDS data were acquired using a SX50 microprobe from Cameca. The results are shown in Fig. 8. EDS and WDS results are found to be consistent with one another within 5%, except for the smallest copper thickness.

Fig. 9 shows the EDS spectra acquired on the four copper thin films. It should be emphasized that EDS analysis of small amounts of copper in nickel is not an easy case because of the partial interference between Cu Kα and Ni Kβ (this interference is of course easily overcome using WDS whose spectral resolution is far better). Nevertheless, it can be observed from Fig. 8 that the copper thickness determination by EDS is very reliable with respect to the WDS one. The discrepancy between the two techniques is actually within 5% apart from the thinnest film, for which the Cu Kα peak height is very small and undoubtedly affected by a high uncertainty (see red spectrum in Fig. 9). Anyway the generally good agreement between the two techniques demonstrates the good reliability of the routine peak deconvolution procedures implemented in most up-to-date EDS software packages.

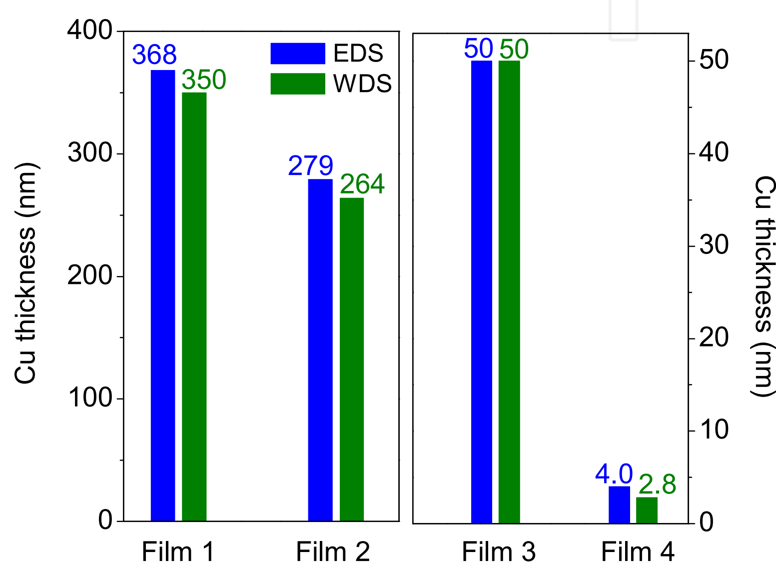

Fig. 8. Thickness determination of a Cu thin film deposited on a nickel substrate by EPMA at 20 kV. Comparison between EDS and WDS.

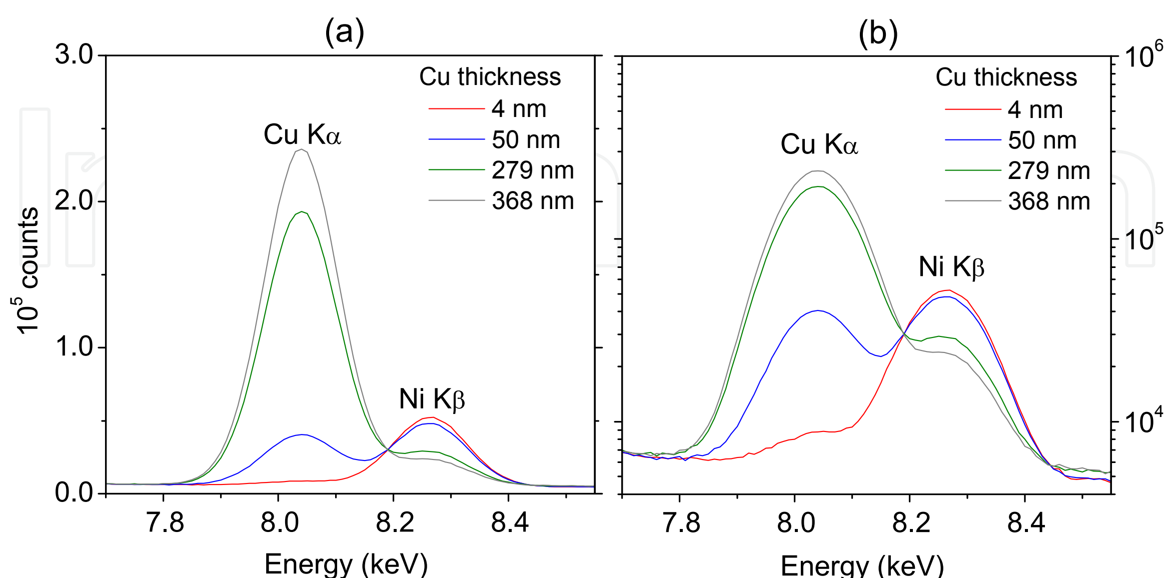

Fig. 9. EDS spectra acquired on four nickel samples coated with different thicknesses of copper. (a) linear counts scale. (b) logarithmic counts scale.

2.5 More complicated samples – Multiple voltage approach

The quantification of thin film thickness in the examples shown in the previous sections is quite easy as both the thin film and substrate compositions are known, and a single voltage approach is sufficient. EPMA-EDS can also be used for the analysis of thin films in more complicated situations including thin films and/or substrates of unknown composition, as well as multilayer structures. In those cases, a multiple voltage approach is usually required. This is out of the scope of this paper but nice examples of such complex samples can be found in (Pouchou & Pichoir, 1993).

3. EPMA-WDS: A tool for the characterization of surface thin films in the monolayer and sub-monolayer range

3.1 Principle

The principle of thin film analysis by EPMA-WDS is exactly the same as the one detailed for EPMA-EDS in the previous section. The difference is that WDS has a much better sensitivity than EDS and hence enables the quantification of much thinner films, down to the submonolayer range. The use of EPMA-WDS for the quantification of such thin layers has been described in details in (Christien & Le Gall, 2008; Nowakowski et al., 2011). For very thin surface layers, the quantification equation (Eq. (2)) can be simplified. As the layer mass thickness μ is very small, Eq. (2) reduces to:

$$\frac{I}{I_{Std}} = \frac{\mu \times \xi(0)}{\int_{\rho z=0}^{\infty} \xi_{Std}(\rho z)\, d\rho z} \tag{4}$$

or, if the standard material is not a pure element:

$$\frac{I}{I_{Std}} = \frac{\mu \times \xi(0)}{X_{Std} \int_{\rho z=0}^{\infty} \xi_{Std}(\rho z)\, d\rho z} \tag{5}$$

where X_{Std} is the weight fraction of the analysed element in the standard material. So in the case of a very thin surface layer, the layer mass thickness μ is simply proportional to the measured k-ratio:

$$\mu = K \frac{I}{I_{Std}} \tag{6}$$

with:

$$K = \frac{X_{Std} \int_{\rho z=0}^{\infty} \xi_{Std}(\rho z)\, d\rho z}{\xi(0)} \tag{7}$$

K can be easily determined for any system at a given beam voltage using the XPP model. Let us consider for example a substrate of nickel covered by a fractional monolayer of sulphur

(the Ni-S system is chosen here as an example as the next sections are devoted to it). Fig. 10 shows the ξ functions for the S Kα line at 20 kV in nickel and in the FeS_2 compound which was used here as a standard material. The sulphur weight fraction in FeS_2 is X_{Std} = 0.534. We finally obtain: K = 256.1 μg cm^{-2} at 20 kV. It should be emphasized that the K constant is voltage-dependant: the higher the beam voltage, the higher the K constant.

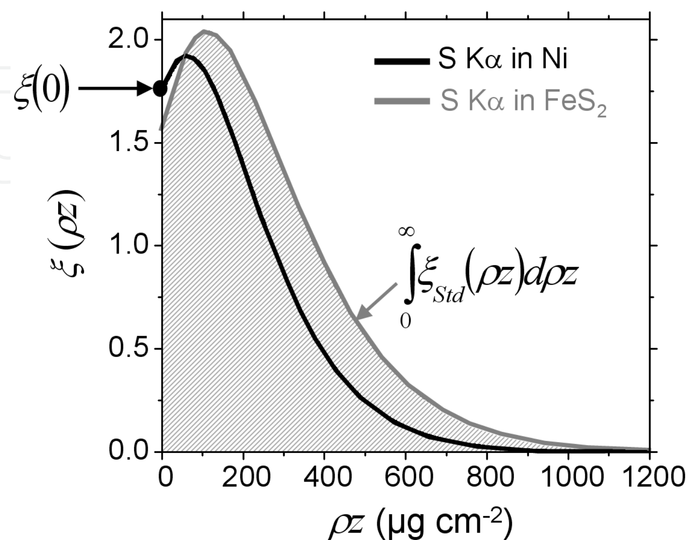

Fig. 10. ξ functions calculated using the XPP model at 20 kV for the sulphur Kα line in nickel and FeS_2 (used in this work as a standard material for sulphur element).

The use of EPMA-WDS to quantify surface monolayers and sub-monolayers is quite recent. It can be of great interest for the investigation of surface and grain boundary segregation phenomena in materials science (Christien & Le Gall, 2008; Nowakowski et al., 2011). The well-known case of sulphur segregation in nickel will be considered in the next sections. Nickel and nickel alloys always contain traces of sulphur at the level of some ppm or tens of ppm. When the material is annealed at an "intermediate" temperature (typically 400°C to 800°C), sulphur atoms tend to gather on the surfaces and at the grain boundaries as a monolayer or fraction of a monolayer. This is what we call "interface segregation" which is a very important metallurgical phenomenon as it can dramatically affect the metal properties (Saindrenan et al., 2002; Lejcek, 2010).

EPMA-WDS data presented in this section were acquired either on a Cameca SX50 microprobe equipped with four WDS spectrometers or on a Carl Zeiss Merlin high current SEM equipped with an Oxford Instrument INCA Wave spectrometer.

3.2 Surface segregation

A nickel sample containing 7.2 wt ppm of sulphur was annealed for 112 h at 800°C under high vacuum and then introduced in the microprobe. After annealing, the surface is expected to be covered by a sulphur fractionnal monolayer because of surface segregation. An example of sulphur Kα peak acquired by EPMA-WDS on that sample at 10 kV is shown in Fig. 11. As demonstrated later, this peak is entirely due to the sulphur fractional monolayer covering the nickel substrate, and not to the sulphur located in the sample bulk. A good peak-to-background ratio is demonstrated, which illustrates the very good sensitivity of WDS.

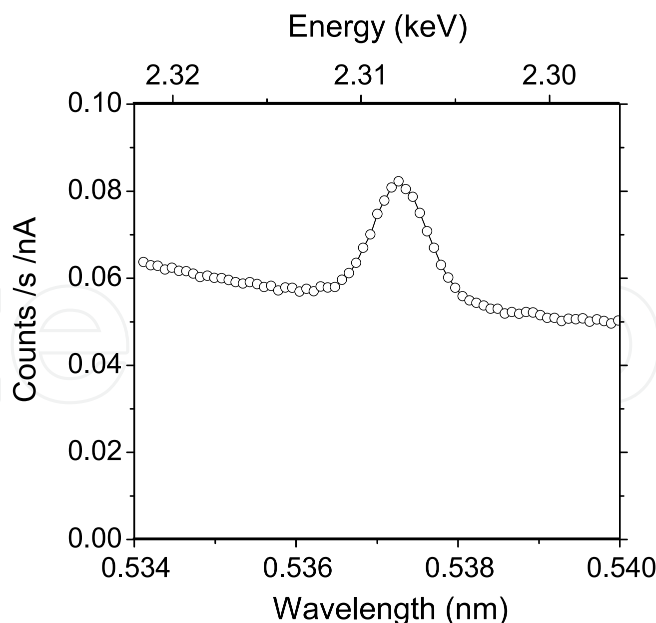

Fig. 11. WDS spectrum of the S Kα line acquired at 10 kV on a nickel sample covered with a fractional monolayer of sulphur.

Fig. 12 shows the voltage-dependence of the S Kα k-ratio measured at the sample surface. The strong decrease of the k-ratio over the beam voltage indicates that the detected sulphur signal is coming from the surface (and not from the bulk). The k-ratio corresponding to the sulphur bulk content (7.2 wt ppm) can be calculated and it is expected to be as low as ~10^{-5} (no matter what the beam voltage is) which is far below the experimental k-ratio values. So the bulk contribution to the sulphur WDS signal measured here can be considered negligible.

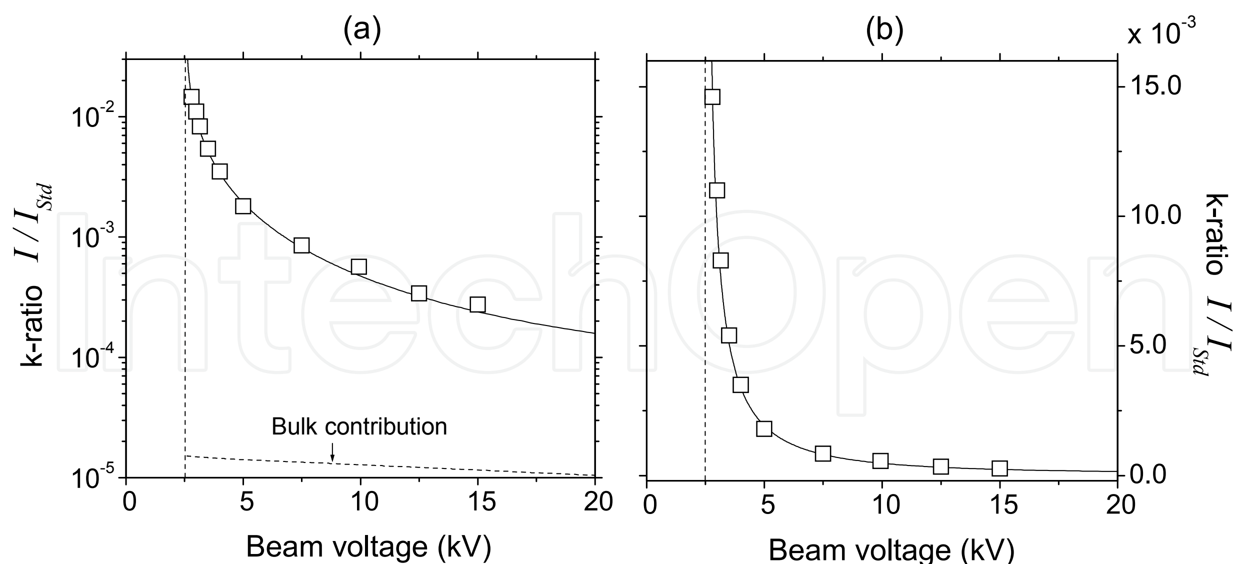

Fig. 12. Beam voltage dependence of the sulphur Kα k-ratio on a nickel substrate covered by a sulphur fractional monolayer. The points are WDS measurements and the curves were calculated using Eq. (5) for beam voltages ranging from 2.5 to 20 kV. (a) logarithmic k-ratio scale. (b) linear k-ratio scale. The dotted vertical line is the sulphur K level energy below which no Kα emission is observed.

The surface sulphur mass thickness μ can be quantified here from the experimental k-ratio measured at any voltage (again, a single-voltage approach would be sufficient here). The μ values determined at the ten different beam voltages investigated here were found to be consistent with each other within 5%. On average, we found:

$$\mu = 42.0 \text{ ng cm}^{-2} \tag{8}$$

This mass thickness can be converted to a number of sulphur atoms. It corresponds to 7.9×10^{14} atoms cm^{-2}, which is about half the density of a (100) nickel plane (1.6×10^{15} atoms cm^{-2}).

3.3 Grain boundary segregation

The conventional route for the analysis of grain boundaries using surface techniques such as Auger spectroscopy is to fracture the sample and to analyse the fractured surface. When elements such as sulphur or phosphorus are segregated, the material usually breaks along the grain boundaries which makes it possible to analyse them using surface analysis techniques. The same procedure was undertaken in this work for EPMA-WDS analysis. Nickel samples containing 5.4 wt ppm of sulphur in bulk were annealed at 550°C, 750°C and 900°C. Each of them was then fractured using tensile test in liquid nitrogen and one half of the broken specimen was introduced into the Merlin SEM chamber for WDS analysis. The WDS analyses were carried out using a beam voltage of 20 kV and a beam current of 400 nA. It should be emphasized that in this work the samples were fractured *ex-situ* with a conventional tensile machine, in contrast to the Auger spectroscopy procedure where the sample *must* be fractured *in-situ* (i.e. in the ultra-high vacuum of the spectrometer chamber) to avoid any surface contamination. Fig. 13a shows the principle of grain boundary segregation analysis by EPMA-WDS and Fig. 13b is one of the fracture surfaces observed in the Merlin SEM. For each of the three samples, about 15 to 20 grain boundary facets were analysed with a counting time of 6 minutes each.

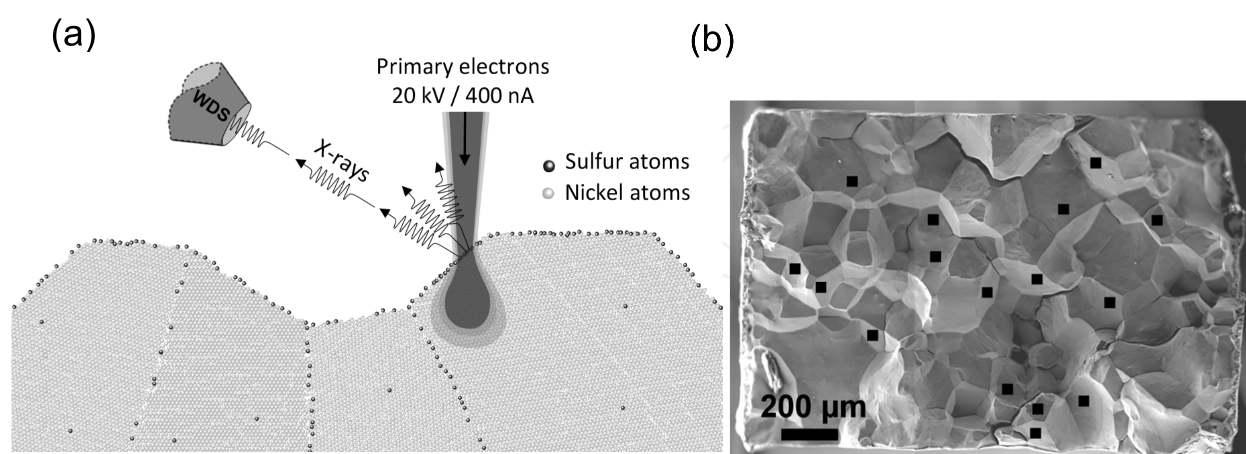

Fig. 13. (a) Principle of grain boundary segregation quantification by EPMA-WDS.
(b) Example of grain boundary fracture surface observed in the SEM and analysed using WDS. The black squares indicate the analysed areas.

One difficulty of this kind of analysis is that the analysed facet is in general not perpendicular to the primary electron beam. In that case, Eq. (6) becomes:

$$\mu = K \frac{I}{I_{Std}} \cos\theta \quad (9)$$

where θ is the tilt angle (i.e. the angle between the facet normal and the primary beam). The tilt angle can be determined for each analysed facet from the measurement of the absorbed specimen current using Eq. (10) (a detailed description of that technique is given in (Nowakowski et al., 2011)):

$$\cos\theta = \frac{0.36}{1 - C_{ABS}/C_B} \quad (10)$$

where C_B is the primary beam current and C_{ABS} is the absorbed specimen current. It should be noticed that the 0.36 constant in Eq. (10) is correct only for a *nickel* sample and at a beam voltage of 20 kV. As the sample is fractured before analysis, the initial sulphur grain boundary concentration is randomly split on both fracture surfaces so that the sulphur concentration detected by WDS is only one half of the initial grain boundary concentration. This has to be taken into account in the quantification equation which becomes:

$$\mu = 2K \frac{I}{I_{Std}} \cos\theta \quad (11)$$

Fig. 14 shows the distributions of the sulphur mass thickness μ over the analysed grain boundary facets for the three nickel samples with different annealing temperatures. It is demonstrated that the average sulphur grain boundary concentration $\bar{\mu}$ significantly decreases with the annealing temperature, which is consistent with the Langmuir-McLean formalism of segregation (Saindrenan et al., 2002; Lejcek, 2010).

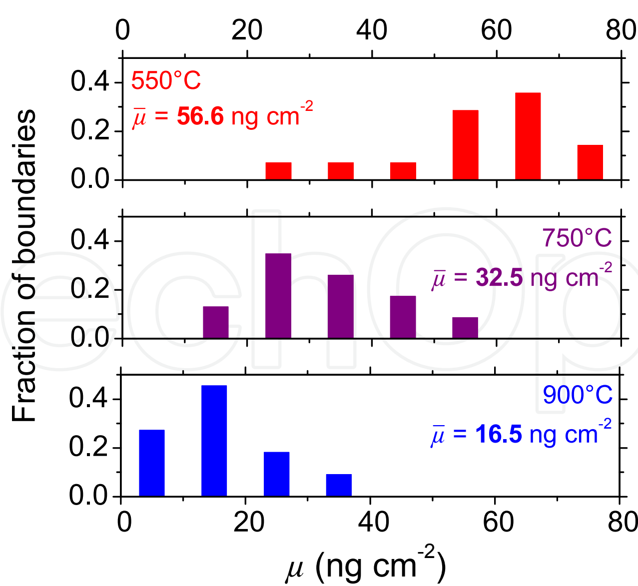

Fig. 14. Distributions of the sulphur concentration μ over the grain boundary facets analysed by EPMA-WDS. The colours correspond to three nickel samples with different annealing temperatures. $\bar{\mu}$ is the sulphur concentration averaged over all the analysed grain boundary facets.

The limit of detection of EPMA-WDS for the analysis of very thin surface layers has been determined in (Christien & Le Gall, 2008). For a primary beam current of 400 nA and a counting time of a few minutes, it is of the order of 1 ng cm^{-2}, which corresponds to about 1% of a monolayer.
The main advantage of EPMA-WDS with respect to Auger spectroscopy (which has been the most common technique for the analysis of interface segregation for decades) is that it is insensitive to surface contamination from the atmosphere. This is due to the "high" energy of Kα X-rays with respect to Auger electrons. For example, in the case of sulphur, the Kα line energy is 2.3 keV. This enables the X-rays to get through the thin contamination layer that forms when the sample is in contact with air (Nowakowski et al., 2011). On the contrary, the sulphur Auger electrons have an energy of 0.15 keV only and are totally absorbed in the atmospheric contamination layer. The consequence is that the sample preparation for Auger analysis has to be done *in-situ* (including cryogenic fracturing of the sample needed for grain boundary segregation analysis), whereas it can be done *ex-situ* for EPMA-WDS analysis, which is a very substantial advantage.

4. EPMA analysis of sandwich films

4.1 Principle

It has been demonstrated in the previous sections that EPMA is a powerful technique for the quantification of surface thin films. That technique can be extended to the case of "sandwich" films, which is a very common configuration in materials science (grain boundary segregation, multilayered structures in microelectronics…) as well as in geology or biology. Let us consider for example a gold sandwich film in a nickel matrix (Fig. 15). The technique consists in preparing a cross-section of material and acquiring an EPMA concentration profile across the film as shown in Fig. 15. The film is assumed thin enough (<~50 nm) to have no significant effect on the electron probe size and shape. In other words, the probe is supposed to be the same as it would be in pure nickel (or in nickel containing a very small concentration of gold).

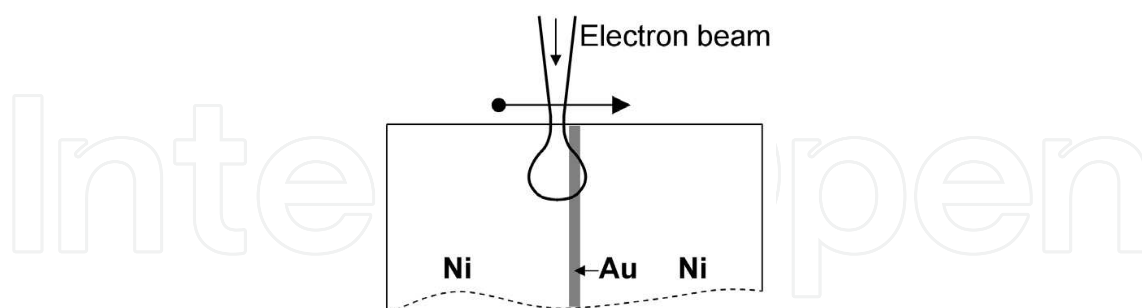

Fig. 15. Principle of EPMA quantification of a sandwich thin film.

As demonstrated in the following, the gold peak that is detected on the concentration profile can be used to quantify the gold mass thickness. The analysed volume V is schematically represented on Fig. 16a. l is the length of the concentration profile and S is the surface of gold film in the analysed volume. A_{Peak} is the peak area measured on the concentration profile (g cm^{-2}) (Fig. 16b).
A general characteristic of microbeam techniques is that an object of real size A analysed with a probe of size B has an "observed" size ~ $A+B$. In our case, the size of the object (the

Au film) is negligible in comparison to the probe size (~ 1000 nm at 20 kV). The "observed" object size is then equal to the probe size. In other words, the peak width observed in the Au concentration profile is not the Au film width, but the electron probe size.

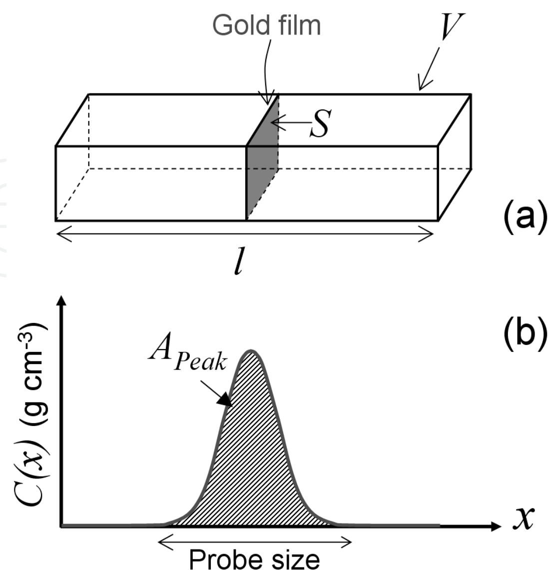

Fig. 16. a) Schematic shape of the volume analysed by EPMA during a profile along the x direction. V is the analysed volume, l is the length of the concentration profile and S is the surface of gold film in the analysed volume. b) Measured gold concentration profile across the film. A_{Peak} is the profile peak area (g cm^{-2}).

The mean gold concentration $\overline{C}$ (g cm^{-3}) over the analysed volume is defined by (Fig. 16b):

$$\overline{C} = \frac{1}{l} \int_{x=0}^{l} C(x)\,dx \tag{12}$$

By definition, the peak area A_{Peak} is:

$$A_{Peak} = \int_{x=0}^{l} C(x)\,dx \tag{13}$$

So that:

$$\overline{C} = \frac{A_{Peak}}{l} \tag{14}$$

Assuming that this mean concentration $\overline{C}$ is originating entirely from the gold film, we can determine the gold mass thickness μ expressed in g cm^{-2}:

$$\mu = \frac{\overline{C} \times V}{S} = \overline{C} \times l \tag{15}$$

From Eqs (14) and (15):

$$\mu = A_{Peak} \tag{16}$$

The Au mass thickness μ (g cm^{-2}) can be converted into an Au thickness (cm), as long as the layer density ρ_{Au} is known:

$$e_{Au} = \frac{\mu_{Au}}{\rho_{Au}} = \frac{A_{Peak}}{\rho_{Au}} \quad (17)$$

4.2 Example

A 23 nm thick Au sandwich film in a nickel matrix was analysed by EPMA-EDS. Fig. 17 shows the experimental EPMA-EDS gold concentration profiles obtained at 15, 20 and 25 kV. Data processing using Eq. (17) gives e_{Au} = 25.6 nm at 15 kV, 26.2 nm at 20 kV and 24.8 nm at 25 kV. The results are in good agreement with the expected value of 23.0 nm. It is interesting to notice also that as expected the result does not depend on the beam voltage.
This technique has been for example used recently to measure gallium sandwich thin films in aluminium obtained by grain boundary penetration of liquid gallium. That work is to be published elsewhere.
The results presented in Fig. 17 are quite exploratory, but very promising. The development of the EPMA technique applied to very thin sandwich films is still in progress. In the near future, it should be possible (especially using WDS rather than EDS) to quantify much thinner sandwich films (down to the monolayer range), which is of great interest for many applications in materials science.

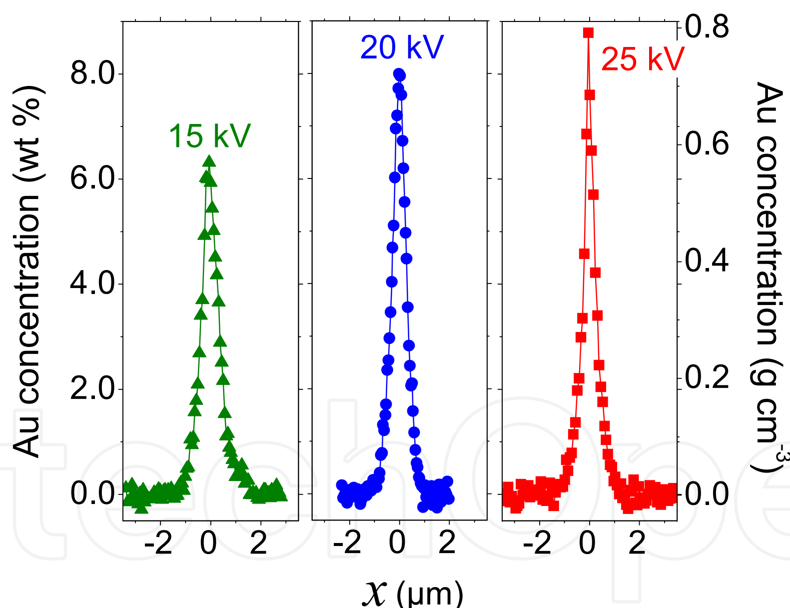

Fig. 17. EPMA-EDS Au concentration profiles acquired on a 23.0 nm thick Au sandwich film in a Ni matrix at 15, 20 and 25 kV.

5. Conclusion

It has been demonstrated in this paper that EPMA can be used to accurately determine the thickness of thin films. Examples have been given demonstrating that EDS is a very simple tool for the quantification of thin films in the range 10 nm to 1000 nm, including in complicated situation involving "light" elements (oxygen) and rough surfaces.

WDS offers much higher sensitivity than EDS and enables the determination of ultra-thin surface layers down to the sub-monolayer range, which makes it a competitive technique for surface analysis with respect to more usual techniques such as Auger spectroscopy. EPMA-WDS has even been very successfully used for the quantification of grain boundary segregation on fractured samples.
"Sandwich" thin films can also be quantified using EPMA. Some preliminary results on a 23 nm thick gold film in a nickel matrix were presented in this work. These promising results show that it should be possible in the near future to quantify sub-monolayer sandwich thin films using EPMA (especially with WDS rather than EDS), which is of great interest for various applications in materials science.

6. Acknowledgements

Vincent Barnier (SMS-MPI, Ecole Nationale Supérieure des Mines de Saint-Etienne) is sincerely acknowledged for careful XPS experiments.

7. References

Bastin G., Heijligers H. & Dijkstra J. (1990). Computer programs for the calculation of X-ray intensities emitted by elements in multiplayer structures. *Proceedings of the 25th Annual Conference of Microbeam Analysis Society,* Seattle, August 1990, pp. 159-160. ISSN: 02781727.

Bauccio M. (2nd Edition) (1994). *ASM Engineered Materials Reference Book*, Ed. ASM International, Materials Park, OH.

Castaing R. & Guinier A. (1950). Application des sondes électroniques à l'analyse métallographique. *Proceedings of First Europ. Conf. Electr. Microscopy,* Delft, July 1949.

Castaing R. (1951). *Application des sondes électroniques à une méthode d'analyse ponctuelle chimique et cristallographique*, Ph. D. Thesis, Université de Paris, France.

Christien F. & Le Gall R. (2008). Measuring surface and grain boundary segregation using wavelength dispersive X-ray spectroscopy. *Surface Science* Vol. 602, pp. 2463-2472.

Ferchaud E. (2010). *Brasage-diffusion de l'aluminium par le gallium.* PhD thesis, Université de Nantes, France

Grillon F. & Philibert J. (2002). The legacy of Raymond Castaing. *Mikrochim. Acta.* Vol. 138, No. 3-4, pp. 99-104. ISSN: 00263672.

Lejcek P. (2010). *Grain Boundary Segregation in Metals*, Springer, ISBN 978-3-642-12504-1.

Llovet X. & Merlet C. (2010). Electron probe microanalysis of thin films and multilayers using the computer program XFILM, *Microscopy and Microanalysis* Vol. 16, pp. 21-32. ISSN: 14319276.

Nowakowski P., Christien F., Allart M., Borjon-Piron Y. & Le Gall R. (2011). Measuring grain boundary segregation using Wavelength Dispersive X-ray Spectroscopy: Further developments. *Surface Science* Vol. 605, pp. 848-858.

Packwood R.H. & Brown J.D. (1981). A Gaussian expression to describe $\phi(\rho z)$ curves for quantitative electron probe microanalysis. *X-Ray Spectrom.*, Vol. 10, pp. 138-146.

Philibert J. & Tixier R. (1968). Electron penetration and the atomic number correction in electron probe microanalysis. Brit. *J. Appl. Phys.* Vol. 1, pp. 685-694. ISSN: 00223727.

Pouchou J.L. & Pichoir F. (1987). Basic expressions of PAP computation for quantitative EPMA, *Proceedings of ICXOM 11*, Ontario, August 1987, pp. 249-253.

Pouchou J.L., Pichoir F. & Boivin D. (1990). XPP procedure applied to quantitative EDS X-ray analysis in the SEM, *Proceedings of the 25th Annual Conference of Microbeam Analysis Society*, Seattle, August 1990, pp. 120-126. ISSN: 02781727.

Pouchou J.L. & Pichoir F. (1991). Quantitative analysis of homogeneous or stratified microvolumes applying the model "PAP", In: *Electron Probe Quantitation* Heinrich K., Newbury D., pp. 31-76, Plenum Press, ISBN 0306438240, 9780306438240, New-York.

Pouchou J.L. (1993). X-Ray microanalysis of stratified specimens, *Anal. Chim. Acta*, Vol. 283, pp. 81-97.

Pouchou J.L. & Pichoir F. (1993). Electron probe X-ray microanalysis applied to thin surface films and stratified specimens, *Scanning Microscopy Supplement*, Vol. 7, pp. 167-189. ISSN: 0892-953X.

Saindrenan G., Le Gall R. & Christien F. (2002) *Endommagement interfacial des métaux*, Editions Ellipses, ISBN 2-7298-0911-2, Paris.

Staub P., Jonnard P., Vergand F., Thirion J. & Bonnelle A.C. (1998). IntriX: A Numerical Model for Electron Probe Analysis at High Depth Resolution: Part II - Tests and Confrontation with Experiments, *X-Ray Spectrom.* Vol. 27, pp. 58-66. ISSN: 00498246

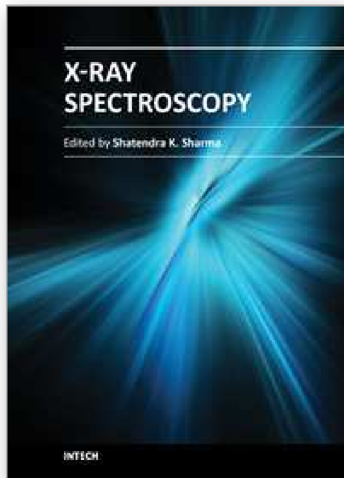

X-Ray Spectroscopy
Edited by Dr. Shatendra K Sharma

ISBN 978-953-307-967-7
Hard cover, 280 pages
Publisher InTech
Published online 01, February, 2012
Published in print edition February, 2012

The x-ray is the only invention that became a regular diagnostic tool in hospitals within a week of its first observation by Roentgen in 1895. Even today, x-rays are a great characterization tool at the hands of scientists working in almost every field, such as medicine, physics, material science, space science, chemistry, archeology, and metallurgy. With vast existing applications of x-rays, it is even more surprising that every day people are finding new applications of x-rays or refining the existing techniques. This book consists of selected chapters on the recent applications of x-ray spectroscopy that are of great interest to the scientists and engineers working in the fields of material science, physics, chemistry, astrophysics, astrochemistry, instrumentation, and techniques of x-ray based characterization. The chapters have been grouped into two major sections based upon the techniques and applications. The book covers some basic principles of satellite x-rays as characterization tools for chemical properties and the physics of detectors and x-ray spectrometer. The techniques like EDXRF, WDXRF, EPMA, satellites, micro-beam analysis, particle induced XRF, and matrix effects are discussed. The characterization of thin films and ceramic materials using x-rays is also covered.

How to reference
In order to correctly reference this scholarly work, feel free to copy and paste the following:

Frédéric Christien, Edouard Ferchaud, Pawel Nowakowski and Marion Allart (2012). The Use of Electron Probe MicroAnalysis to Determine the Thickness of Thin Films in Materials Science, X-Ray Spectroscopy, Dr. Shatendra K Sharma (Ed.), ISBN: 978-953-307-967-7, InTech, Available from: http://www.intechopen.com/books/x-ray-spectroscopy/the-use-of-electron-probe-microanalysis-to-determine-the-thickness-of-thin-films-in-materials-scienc

INTECH
open science | open minds

InTech Europe
University Campus STeP Ri
Slavka Krautzeka 83/A
51000 Rijeka, Croatia
Phone: +385 (51) 770 447
Fax: +385 (51) 686 166
www.intechopen.com

InTech China
Unit 405, Office Block, Hotel Equatorial Shanghai
No.65, Yan An Road (West), Shanghai, 200040, China
中国上海市延安西路65号上海国际贵都大饭店办公楼405单元
Phone: +86-21-62489820
Fax: +86-21-62489821

© 2012 The Author(s). Licensee IntechOpen. This is an open access article distributed under the terms of the Creative Commons Attribution 3.0 License, which permits unrestricted use, distribution, and reproduction in any medium, provided the original work is properly cited.

IntechOpen

IntechOpen